Time-Resolved Optical and Infrared Spectral Studies of Intermediates Generated by Photolysis of *trans*-RhCl(CO)(PR_3)$_2$. Roles Played in the Photocatalytic Activation of Hydrocarbons[1]

Jon S. Bridgewater,[†] Thomas L. Netzel,[‡] Jon R. Schoonover,[§] Steven M. Massick,[†] and Peter C. Ford*,[†]

Department of Chemistry, University of California, Santa Barbara, California 93106, Department of Chemistry, Georgia State University, Atlanta, Georgia, and Polymers and Coatings Group, Material Science and Technology Division, Los Alamos National Laboratory, Los Alamos, New Mexico 87545

Received November 16, 2000

Described are picosecond and nanosecond time-resolved optical (TRO) spectral and nanosecond time-resolved infrared (TRIR) spectral studies of intermediates generated when the rhodium(I) complexes *trans*-RhCl(CO)L_2 (L = PPh_3 (**I**), P(*p*-tolyl)$_3$ (**II**), or PMe_3 (**III**)) are subjected to photoexcitation. Each of these species, which are precursors in the photocatalytic activation of hydrocarbons, undergoes CO labilization to form an intermediate concluded to be the solvated complex RhCl(Sol)L_2 ($\mathbf{A_i}$). The picosecond studies demonstrate that an initial transient is formed promptly (<30 ps), which decays to $\mathbf{A_i}$ with lifetimes ranging from 40 to 560 ps depending upon L and the medium. This is proposed on the basis of ab initio calculations to be a metal-to-ligand charge transfer (MLCT) excited state. Second-order rate constants (k_{CO}) for reaction of the $\mathbf{A_i}$ with CO were determined, and these depend on the nature of L and the solvent, the slowest rate being for $\mathbf{A_I}$ in tetrahydrofuran ($k_{CO} = 7.1 \times 10^6$ M^{-1} s^{-1}), the fastest being for $\mathbf{A_{III}}$ in dichloromethane (1.3×10^9 M^{-1} s^{-1}). Each $\mathbf{A_i}$ also undergoes competitive unimolecular reaction with solvent to form long-lived transients with TRIR properties suggesting these to be Rh(III) products of oxidative addition. Although this was mostly suppressed by the presence of higher concentrations of CO (which trapped $\mathbf{A_i}$ to re-form the starting complexes in each case), both TRO and TRIR experiments indicate that a fraction of the oxidative addition could not be quenched. Thus, the short-lived MLCT state or a vibrationally hot species formed during the decay of this excited state appears to participate directly in C−H activation.

Introduction

The selective catalytic functionalization of saturated hydrocarbons is a goal with considerable economic importance with respect to the conversion of low-value alkanes to higher value functionalized analogues.[2] The difficulty in selectively activating alkanes can be attributed to the high bond dissociation energies and low acidities and basicities of carbon−hydrogen bonds. Nonetheless, pathways for activating C−H bonds via free radical abstraction by reaction with strong electrophiles and by oxidative addition to low-valent transition metal centers in homogeneous solutions have been described.[2−4] The oxidative addition pathway has the potential to be highly selective, but examples of hydrocarbon functionalization by this route generally have not proved catalytic. In this context, reports that rhodium(I) complexes of the type *trans*-RhCl(CO)L_2 (L = PR_3, a trialkyl or triaryl phosphine) may be precursors to catalytic or photocatalytic species for the functionalizations of various hydrocarbons[5,6] have drawn considerable experimental[5−9] and theoretical[10] attention. Described here are the results of nanosecond laser flash photolysis studies using time-resolved infrared (TRIR) and time-resolved optical (TRO) detection to probe the nature of reactive intermediates generated by the photolysis of RhCl(CO)(PPh_3)$_2$ (**I**), RhCl(CO)(P(p-tolyl)$_3$)$_2$ (**II**), and RhCl-

[†] University of California.
[‡] Georgia State University.
[§] Los Alamos National Laboratory.

(1) (a) Taken in part from the Ph.D. Dissertation of J. S. Bridgewater, University of California, Santa Barbara, 1998. (b) Preliminary reports of aspects of this work appeared in refs 1c and 1d. (c) Bridgewater, J. S.; Lee, B.; Bernhard, S.; Schoonover, J. R.; Ford, P. C. *Organometallics* **1997**, *16*, 5592−5594. (d) Ford, P. C.; Netzel, T. L.; Spillett, C. T.; Pourreau, D. B. *Pure Appl. Chem.* **1990**, *62*, 1091−1094.
(2) (a) Armdtsen, B. A.; Bergman, R. G.; Mobley, T. A.; Peterson, T. H. *Acc. Chem. Res.* **1995**, *28*, 154−162. (b) Bergman, R. G. *Science* **1984**, *223*, 902.
(3) Shilov, A. E.; Shulpin, G. B. *Chem. Rev.* **1997**, *97*, 2879−2932.
(4) Crabtree, R. H. *Chem. Rev.* **1985**, *85*, 245.
(5) (a) Kunin, A. J.; Eisenberg, R. *J. Am. Chem. Soc.* **1986**, *108*, 535−536. (b) Kunin, A. J.; Eisenberg, R. *Organometallics* **1988**, *7*, 2124−2129.
(6) (a) Sakakura, T.; Tanaka, M. *Chem. Commun.* **1987**, 758−759. (b) Sakakura, T.; Sodeyama, T.; Tanaka, M. *New J. Chem.* **1989**, *13*, 737−745. (c) Sakakura, T.; Sodeyama, T.; Sasaki, K.; Wada, K.; Tanaka, M. *J. Am. Chem. Soc.* **1990**, *112*, 7221−7229.
(7) (a) Maguire, J. A.; Boese, W. T.; Goldman, A. S. *J. Am. Chem. Soc.* **1989**, *111*, 7088−7093. (b) Boese, W. T.; Goldman, A. S. *J. Am. Chem. Soc.* **1992**, *114*, 350−351. (c) Shih, K. C.; Goldman, A. S. *Organometallics* **1993**, *12*, 3390−3392. (d) Rosini, G. P.; Boese, W. T.; Goldman, A. S. *J. Am. Chem. Soc.* **1994**, *116*, 9498−9505. (e) Rosini, G. P.; Soubra, S.; Vixamar, M.; Wang, S. Y.; Goldman, A. S. *J. Organomet. Chem.* **1998**, *554*, 41−47. (f) Rosini, G. P.; Liu, F. C.; Krogh-Jespersen, K.; Goldman, A. S.; Li, C. B.; Nolan, S. P. *J. Am. Chem. Soc.* **1998**, *120*, 9256−9266
(8) (a) Iwamoto, A.; Itagaki, H.; Saito, Y. *J. Chem. Soc., Dalton Trans.* **1991**, 1093−1097. (b) Matsubara, T.; Saito, Y. *J. Mol. Catal.* **1994**, *92*, 1−8.
(9) (a) Boyd, S. E.; Field, L. D.; Partridge, M. G. *J. Am. Chem. Soc.* **1994**, *116*, 9492−9497. (b) Partridge M. G.; Field, L. D.; Messerle, B. A. *Organometallics* **1996**, *15*, 872−877.
(10) (a) Sakaki, S.; Ujino, Y.; Sugimoto, M. *Bull. Chem. Soc. Jpn.* **1996**, *69*, 3047−3057. (b) Margl, P.; Ziegler, T.; Blöchl, P. E. *J. Am. Chem. Soc.* **1995**, *117*, 12625−12634; **1996**, *118*, 5412−5419. (c) Koga, N.; Morokuma, K. *J. Am. Chem. Soc.* **1993**, *115*, 6883−6892.

10.1021/ic001298x CCC: $20.00
Published on Web 02/28/2001

$(CO)(PMe_3)_2$ (**III**). Also described are limited picosecond TRO studies designed to probe the early stages of reactions after excitation of the $RhCl(CO)L_2$ substrates.

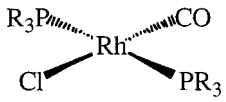

I: $PR_3 = PPh_3$
II: $PR_3 = P(p\text{-tolyl})_3$
III: $PR_3 = PMe_3$

The photoysis of $RhCl(CO)L_2$ was first studied in this laboratory[11] using conventional xenon flash lamp techniques to generate the "tricoordinate" species $RhCl(PPh_3)_2$ proposed to be the key intermediate responsible in H_2 activation by Wilkinson's catalyst $RhCl(PPh_3)_3$ (**IV**).[12] Subsequently, a series of observations based on product studies have indicated that the photochemistry of the $RhCl(CO)L_2$ complexes ($L = PR_3$) is even richer than the reversible CO dissociation and competitive trapping of ligands described above. Indeed, Eisenberg et al.[5] demonstrated using continuous photolysis techniques that the C−H carbonylation product PhCHO is formed as a low quantum yield product when $L = PPh_3$ (eq 1). Additionally, Tanaka et al., Goldman et al., and others have demonstrated that changing L to a trialkyl phosphine such as PMe_3 leads to much greater photochemical reactivity toward C−H activation, including the activation of alkanes.[5−9] There were hints of the C−H activation pathways in the early microsecond flash photolysis studies of **I** by Wink et al.,[11] and a subsequent xenon flash study by Spillett et al.[13] suggested that there were significant differences in the reactivities of intermediates or excited states generated from various $RhCl(CO)L_2$. The present study is an extension of the flash photolysis studies using laser flash techniques with much shorter time resolutions and markedly improved s/n properties.

$$C_6H_6 + CO \xrightarrow{h\nu,\ RhCl(CO)L_2} C_6H_5CHO \qquad (1)$$

Experimental Section

Materials. All solvents used for synthesis were reagent grade, purchased from Aldrich, and distilled over CaH_2 under dinitrogen except where noted. Solvents used for laser flash photolysis were Burdick & Jackson or Aldrich spectroscopic grade and were distilled by following literature procedures.[14] Deuterated solvents were obtained from Cambridge Isotope Laboratories and were used as received. Absolute ethanol was purchased from Quantum Chemical Company and used as received. The $RhCl_3 \cdot 3H_2O$ for syntheses was provided on loan by Johnson-Matthey, Inc. Wilkinson's catalyst $RhCl(PPh_3)_3$ was purchased from Aldrich and was stored in and dispensed from an inert atmosphere glovebox. All other reagents were purchased from Aldrich and used as received.

All gases used for laser flash photolysis experiments were passed through an Oxyclear oxygen scrubber and an indicating oxygen trap (Alltech Associates) prior to use. Gases used in synthesis were passed through a column of 4 Å molecular sieves and Drierite as well as a chromium silica gel column to remove adventitious water or oxygen. Prepurified chromatography grade (99.998%) argon was used in the glovebox and for laser flash photolysis studies. Reagent-grade CO was used for synthesis, and research grade (99.5%) CO (Liquid Carbonics or Spectra Gas) was used in laser flash photolysis studies. Various specialty CO/Ar mixtures of research-grade (99.5%) gases were purchased from Liquid Carbonics and used in laser flash photolysis experiments.

The phosphine complexes $RhCl(CO)(PPh_3)_2$ (**I**) and $RhCl(CO)(P(p\text{-tolyl})_3)_2$ (**II**) were prepared from $RhCl_3$ in high yield according to literature methods.[15] $RhCl(CO)(PMe_3)_2$ (**III**) was synthesized by an adaptation of Crabtree's procedure.[16] Deaerated and dried tetrahydrofuran (THF, ∼30 mL) was transferred by cannula into a round-bottom flask with a 1.7 mmol sample of solid $[Rh(cod)Cl]_2$ (cod = cyclooctadiene) prepared in this laboratory. This solution was entrained with CO for 30 min, then 4 equiv of PMe_3 were added dropwise, and the solution was stirred for 15 min longer. The product was isolated by evaporating the THF under reduced pressure and then recrystallized from toluene layered with hexane.

Instrumentation. Electronic absorption spectra were recorded for solutions in 1.0 cm path length quartz cells using a Hewlett-Packard 8452A diode array and Cary 118 (OLIS digital upgrade) spectrophotometers. Infrared spectra were recorded with a Bio-Rad FTS-60 FTIR spectrophotometer.

Photolysis Solutions. Solutions for photochemical studies were prepared under deaerated conditions using Schlenk techniques and entrained with the appropriate gas. For TRO studies, the sample cell was a 1 cm path length square quartz fluorescence cell which had been modified for attachment to vacuum lines. For TRIR studies, a syringe pump flow system was used to pass the sample solution (2 mL/min) through a modified McCarthy infrared sample cell with a 0.5 mm path length equipped with UV-grade CaF_2 windows. All solutions were studied under flowing conditions in order to avoid repetitive excitation of the small sample volume in the IR cell during multiple pulse averaging data collection. A more detailed description of the flow system can be found elsewhere.[17]

Flash Photolysis Instrumentation. Two systems were used for nanosecond time-resolved optical (TRO) absorption observations at UCSB. The first employed a photomultiplier tube (PMT) detector to obtain kinetic traces at a single monitoring wavelength (λ_{mon}).[18] TRO spectra were recorded at different λ_{mon}, and the individual kinetics traces were laminated together to give three-dimensional time−wavelength−absorbance surfaces. The second system used a CCD camera to record transient spectra at specified delay times.[19] The pump source for all UV/visible transient absorption studies was the frequency-tripled (irradiation wavelength $\lambda_{irr} = 355$ nm) output of a Continuum N-61 Nd:YAG pulsed laser with the power attenuated to ∼20 mJ/pulse and pulse widths ∼10 ns. For kinetics traces and point-by-point transient spectra, the probe beam was the output from an ILC Technology Model R300-5 300W xenon lamp passed through an IR filter and a high-throughput Spex monochromator. The probe and pump beams were approximately collinear and were passed through a SPEX Model 1680 Doublemate dual-grating monochromator after the sample to descriminate against the latter before detection at the RCA 8852 PMT. The PMT output was recorded by a Tektronix TDS 540 digital oscilloscope and transferred to a computer for data analysis and storage.

For CCD experiments, the probe beam was output from an Osram Xenophot HLX lamp perpendicular to the excitation beam. This was focused onto the sample, collected, refocused onto a fiber optic, and brought to a SpectraPro-275 monochromator from Acton Research Corporation. The probe light was then gated by a MCP intensifier,

(11) (a) Wink, D.; Ford, P. C. *J. Am. Chem. Soc.* **1985**, *107*, 1794−1796. (b) Wink, D. A.; Ford, P. C. *J. Am. Chem. Soc.* **1987**, *109*, 436−442.
(12) (a) Halpern, J.; Wong, C. S. *J. Chem. Soc., Chem. Commun.* **1973**, 629. (b) Collman, J. P.; Hegedus, L. S.; Norton, J. R.; Finke, R. G. *Principles and Applications of Organo-transition Metal Chemistry*; University Science Books: Mill Valley, CA, 1987; Chapter 10. (c) Halpern, J. *Inorg. Chim. Acta* **1981**, *50*, 11−19.
(13) Spillett, C. T.; Ford, P. C. *J. Am. Chem. Soc.* **1989**, *111*, 1932−1933.
(14) (a) Riddick, J. A.; Bunger, W. B.; Sakano, T. K. *Organic Solvents: Physical Properties and Methods of Purification*; John Wiley & Sons: New York, 1986. (b) Perrin, D. D.; Armarego, W. L. F.; Perrin, D. R. *Purification of Laboratory Chemicals*; Pergamon Press: Oxford, U.K., 1980.
(15) Collman, J. P.; Sears, C. T.; Kubota, M. *Inorg. Synth.* **1968**, *11*, 99−104.
(16) Burk, M. J.; Crabtree, R. H. *Inorg. Chem.* **1986**, *25*, 931.
(17) Ryba, D. W. Ph.D. Dissertation, University of California, Santa Barbara, 1991.
(18) Crane, D. R.; Ford, P. C. *J. Am. Chem. Soc.* **1991**, *113*, 8510−8516.
(19) (a) Lindsay, E.; Ford, P. C. *Inorg. Chim. Acta* **1996**, *242*, 51−56. (b) Lorkovic, I. M., Miranda, K. M.; Lee, B.; Bernhard, S.; Schoonover, J. R.; Ford, P. C. *J. Am. Chem. Soc.* **1998**, *120*, 11674−11683.

which was run from a PG-200 programmable pulse generator from Princeton Instruments, Inc. The gated light was imaged onto a liquid nitrogen cooled Princeton Instruments Model 1024-EUV CCD, from which data were transferred to a computer. Transients were commonly recorded as 100-shot averages.

Flash photolysis studies with picosecond TRO detection (time resolution ~30 ps) were carried out on a picosecond laser system at the Amoco Research Center, Naperville, IL, built according to a published design.[20] The sample was held in a 50 mL reservoir in a flow system and continuously flowed through a 1 cm path length optical cell. Photolysis at 355 nm was produced with 2.0 mJ pulses of 25 ps duration collimated to a 2 mm diameter beam. Lower pulse energies yielded the same kinetics, but with reduced signal-to-noise ratios.

Two systems were also used for the accumulation of time-resolved infrared (TRIR) spectra. The UCSB apparatus for tunable single-frequency detection (2150 to 1550 cm^{-1}) has been described in detail elsewhere.[21] In the present case the excitation source was the third harmonic of a Lumonics HY600 Nd:YAG laser (λ_{irr} = 355 nm, 20 mJ/pulse, 10 ns pulse width operating at 2 Hz). Some TRIR experiments were performed at LANL using a step-scan FTIR spectrometer with the third harmonic of a Nd:YAG laser (355 nm, 10 ns pulses at 10 Hz) as the excitation source.[22] The time resolution of this kinetics system was ~250 ns.

Low-Temperature Photolyses. Low-temperature FTIR experiments were carried out using a PFD-FT12.5 Pourfill Dewar (R. G. Hansen and Associates) with a sample IR cell built to fit a Bio-Rad FTS-60 FTIR spectrometer. The CaF_2 windows of the sample cell were glued to the brass cell housing, and the cell was sealed by creating an indium O-ring in a tongue-and-groove channel cut into the housing. Solutions (~2×10^{-3} M) for low-temperature IR experiments were prepared under argon and transferred to the deaerated cell using a gastight syringe. Initial FTIR spectra were measured at room temperature and again at low temperature by filling the Dewar with dry ice/acetone or LN_2. The sample was irradiated with 5−10 excimer laser pulses (λ_{irr} = 308 nm), and spectra were collected to monitor formation and decay of intermediates and formation of products.

Computations. Ab initio calculations on *trans*-RhCl(CO)$(PH_3)_2$ were carried out using the COLUMBUS program.[23] This program consists of two components, I43210, which calculates integrals, and S43210, which does the self-consistent field (SCF) minimizations. The I43210 program calculates the one-electron integrals due to nuclear attraction, kinetic energy, overlap, and repulsions due to the core electrons. I43210 also calculates the two-electron integrals due to the Coulombic and exchange integrals for valence shell electrons. The S43210 program performs a Hartree−Fock SCF calculation minimizing the energy for a given electronic configuration and fixed geometry. The total energy is calculated in terms of shell-averaged one-electron, coulomb and exchange integrals. (See additional details below.)

Results

TRO Studies of *trans*-RhCl(CO)$(PPh_3)_2$ (I) in Benzene. Figure 1 displays the optical spectrum of **I** as well as the spectra of two transients, $\mathbf{A_I}$ and $\mathbf{B_I}$, recorded using a CCD camera following laser flash photolysis. The spectrum of shorter lived transient $\mathbf{A_I}$ was recorded immediately (50 ns) after laser excitation (355 nm, 10 ns pulses) with the CCD TRO setup

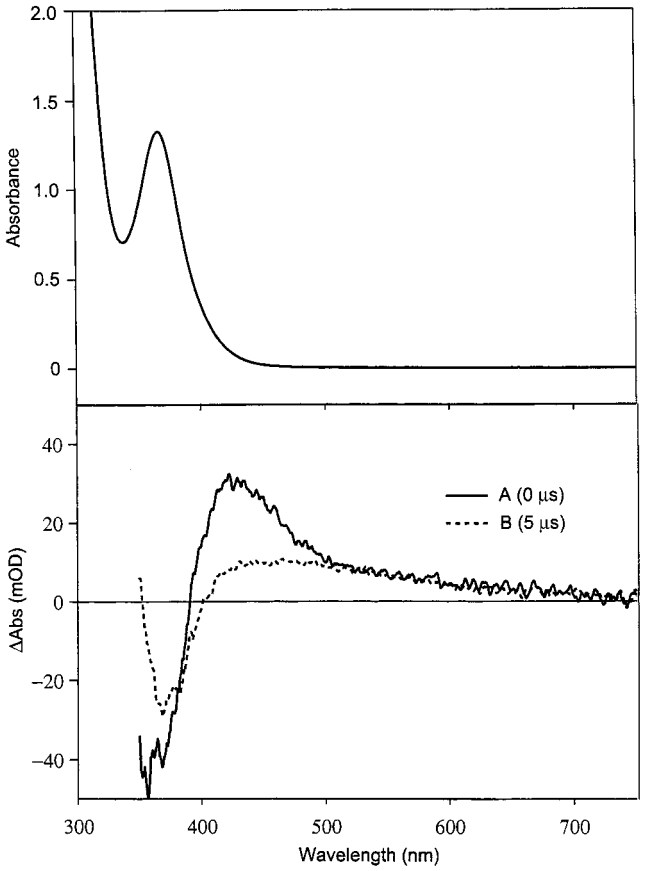

Figure 1. Upper: Electronic absorption spectrum of *trans*-RhCl(CO)-$(PPh_3)_2$ in benzene. Lower: Transient spectra recorded using a CCD camera immediately (A) and 5 μs after (B) a 355 nm flash, each recorded with a 100 ns gatewidth ([**I**] = 0.16 mM, [CO] = 1.5 mM).

(100 ns gate width). This shows a broad increased absorbance relative to the parent compound over the ~390−650 nm range with a maximum absorbance change (ΔAbs) at 420 nm and a maximum bleach at 360 nm. The spectrum of longer lived transient $\mathbf{B_I}$, recorded 5 μs after laser excitation (Figure 1), has increased absorbance over the 405−650 nm range with maximum ΔAbs at ~450 nm and maximum bleach at 380 nm, relative to the ground state. Qualitatively, the same spectral characteristics were seen under either argon or carbon monoxide, although, temporal behavior was a function of the conditions.

Figure 2 illustrates analogous TRO data obtained by using the PMT to record temporal absorbance traces at individual monitoring wavelengths (λ_{mon}) and laminating these traces together to construct three-dimensional representations of ΔAbs vs λ_{mon} vs time for **I**. It can clearly be seen that $\mathbf{A_I}$ forms immediately following the flash, then decays over some microseconds to reveal $\mathbf{B_I}$. The spectral characteristics seen in Figure 2 match the CCD data shown in Figure 1.

Figure 3 illustrates temporal absorbance changes at λ_{mon} = 450 nm following 355 nm flash photolysis (10 ns pulses) of **I** in benzene with added CO (1.3 mM). The fast decay was fitted to an exponential function, and the resulting k_{obs} values were found to increase with increasing [CO]. The plot of k_{obs} versus [CO] (Figure 4) is linear, with a slope (k_{CO}) of (7.8 ± 0.7) × 10^8 M^{-1} s^{-1} and a relatively small nonzero intercept of (1.5 ± 0.3) × 10^5 s^{-1}.[24] The k_{CO} values at different temperatures gave a linear Eyring plot, from which were derived $\Delta H^{\ddagger}$ = 17 ± 4 kJ/mol and $\Delta S^{\ddagger}$ = −34 ± 13 J mol^{-1} K^{-1}.

(20) Winkler, J. R.; Netzel, T. L.; Creutz, C.; Sutin, N. *J. Am. Chem. Soc.* **1987**, *109*, 2381−2392.

(21) (a) McFarlane, K. L. Ph.D. Dissertation, University of California, Santa Barbara, 1996. (b) DiBenedetto, J.; Ryba, D. W.; Ford, P. C. *Inorg. Chem.* **1989**, *28*, 3503−3507. (c) Ford, P. C.; DiBenedetto, J. A.; Ryba, D. W.; Belt, S. T. *SPIE Proc.* **1992**, *1636*, 9−16. (d) Boese, W. T.; Ford, P. C. *J. Am. Chem. Soc.* **1995**, *117*, 8381−8391.

(22) Schoonover, J. R.; Strouse, G. F.; Omberg, K. M.; Dyer, R. B. *Comments Inorg. Chem.* **1996**, *18*, 165−188.

(23) (a) Shephard, R.; Shavitt, I.; Pitzer, R. M.; Comeau, D. C.; Pepper, M.; Lishka, H.; Szalay, P. G.; Ahlrichs, R.; Brown, F. B.; Zhao, J. G. *Int. J. Quantum Chem., Quantum Chem. Symp.* **1988**, *22*, 149−165. (b) Application details appear in: Simon, J. A., Ph.D. Dissertation, University of California, Santa Barbara, 1994. And in: Simon, J. A.; Palke, W. E.; Ford, P. C. *Inorg. Chem.* **1996**, *35*, 6413.

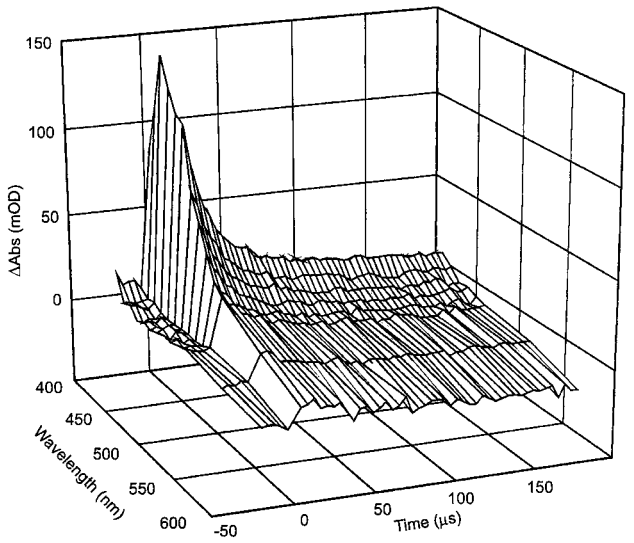

Figure 2. Three-dimensional TRO spectrum for *trans*-RhCl(CO)-$(PPh_3)_2$ in benzene ([**I**] = 0.2 mM, λ_{ex} = 355 nm, under Ar).

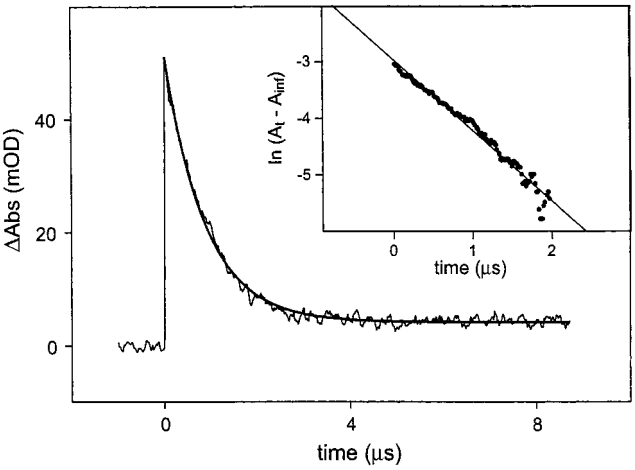

Figure 3. Temporal decay of the transient formed after laser flash photolysis of *trans*-RhCl(CO)$(PPh_3)_2$ in benzene. Inset shows a first-order fit to the data: $k_{obs} = (1.2 \pm 0.1) \times 10^6$ s^{-1} (λ_{ex} = 355 nm, λ_{mon} = 450 nm, [**I**] = 0.28 mM, [CO] = 1.3 mM).

In this context we offer the working hypothesis that $\mathbf{A_I}$ is the "tricoordinate" species "RhCl$(PPh_3)_2$" formed promptly by CO photodissociation from **I** (eq 2, L = PPh_3, $\mathbf{A_i} = \mathbf{A_I}$).

$$\textit{trans}\text{-RhCl(CO)L}_2 \xrightarrow{h\nu} \text{"RhClL}_2\text{"} + \text{CO} \qquad (2)$$

$\mathbf{A_i}$; k_{co}[CO]

Under argon the decay at 450 nm was best fit when the data were analyzed in terms of two first-order decays (supplemental Figure S-1), the faster process with $k = 1.0 \times 10^5$ s^{-1}, the slower with $k = 1.4 \times 10^3$ s^{-1}. The former is in reasonable agreement with the intercept determined from the plot of k_{obs} vs [CO]. Owing to the large difference between the two k's, these data cannot be used to differentiate between a situation where $\mathbf{A_I}$ and $\mathbf{B_I}$ are both formed promptly then decay back to **I** by independent parallel pathways or a mechanism where the reactions occur sequentially, i.e., $\mathbf{A_I} \rightarrow \mathbf{B_I} \rightarrow \rightarrow \mathbf{I}$. Since the decay of $\mathbf{A_I}$ must include a contribution from the second-order reaction with photolabilized CO, the failure to detect this in functional curve fitting such as Figure S-1 illustrates the danger of overinterpreting such fits without examining other parameters, in this case, [CO]. The modest residual ΔAbs in Figure 3 corresponds to absorption attributed largely to $\mathbf{B_I}$, which decays to **I** via slower, CO-independent, processes. Given that **I** participates in photocatalytic benzene carbonylation,[5] a logical candidate for $\mathbf{B_I}$ would be the product of oxidative addition of a benzene or a ligand phenyl ring (orthometalation). The amount of $\mathbf{B_I}$ formed in the flash experiment varies with [CO], decreasing as CO is increased, but approaches a nonzero limit at high CO concentration (Figure 5). We interpret this behavior in terms of competition between second-order trapping of $\mathbf{A_I}$ by CO and (pseudo) first-order C−H activation of either solvent benzene or a ligand to give $\mathbf{B_I}$ (Scheme 1). The failure to quench completely the formation of $\mathbf{B_I}$ suggests that some of this species

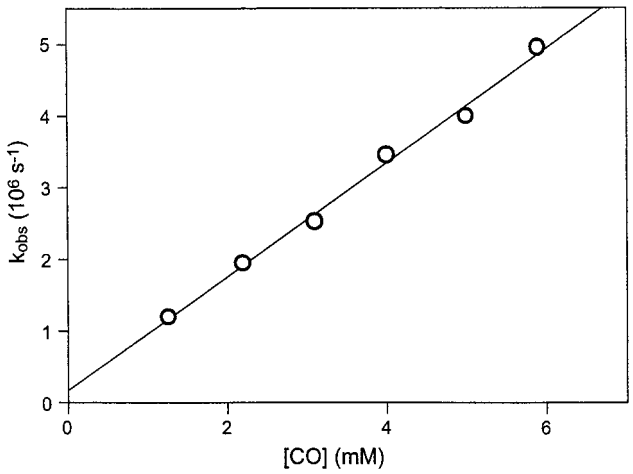

Figure 4. Plot of k_{obs} vs [CO] for the decay of transient $\mathbf{A_I}$ in benzene. For this experiment the values of the slope (k_{CO}) and the intercept were, respectively, 7.8×10^8 M^{-1} s^{-1} and 1.5×10^5 s^{-1} ([**I**] = 0.28 mM, λ_{mon} = 450 nm, 22 °C).

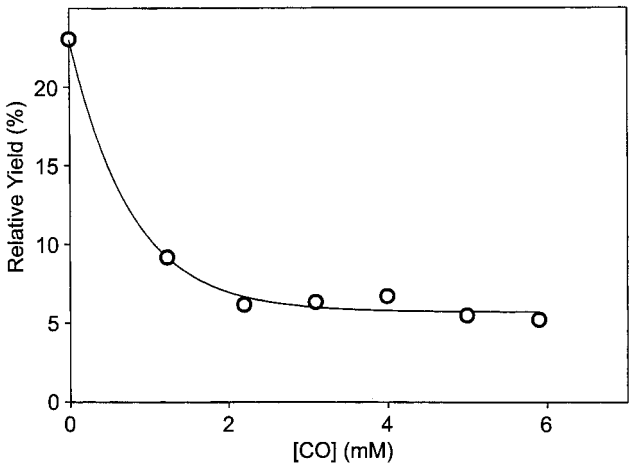

Figure 5. Plot of the relative yield of transients $\mathbf{B_I}$ plus $\mathbf{C_I}$ vs [CO]. A monoexponential decay, $y_i = ae(^{-kx_i}) + c$, was used to model the curve shown. "Relative yield" is defined as (ΔAbs(50 μs)/ΔAbs(50 ns)) × 100 at λ_{mon} = 450 nm ([**I**] = 0.28 mM, T = 22 °C, solvent = benzene).

(24) An earlier microsecond xenon flash lamp photolysis study of **I** in this laboratory[12] reported $k_{CO} = 6.9 \times 10^7$ M^{-1} s^{-1} for the decay of $\mathbf{A_I}$ in benzene. The spectral differences and kinetics observations made in the present study are largely consistent with those of the earlier study, so the 10-fold difference of k_{CO} is puzzling. Careful reexamination of the original data revealed no obvious discrepancies with the results reported here, and it is our conclusion that the error may be the result of a 10% CO tank being inadvertently used instead of a 100% CO tank. It was common practice in this laboratory to achieve desired [CO] by using different CO/Ar mixtures; accidental use of the wrong mixture could account for this error.

Scheme 1

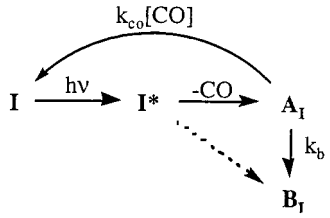

Scheme 2

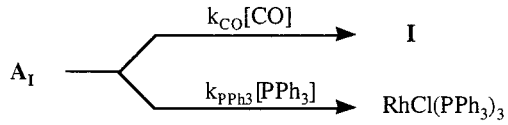

may be formed promptly either from the electronic excited state or from a vibrationally "hot" state of **I** resulting from the decay of **I***.

Under argon, the decay of $\mathbf{B_I}$ reveals a third, even longer lived, transient absorbance ($\mathbf{C_I}$) at 450 nm (supplemental Figure S-2), but this was too long-lived (>50 ms) to be probed with the current setup owing to diffusion out of the excitation volume. However, since the spectrum of a benzene solution of **I** did not change after repetitive laser flashes (1000 shots at 2 Hz), $\mathbf{C_I}$ must also eventually decay to re-form **I**. This is consistent with published results stating that little net photochemistry was observed after continuous photolysis under anaerobic conditions.[25] $\mathbf{C_I}$ was not observed in the TRO studies under added CO; thus $\mathbf{A_I}$ is the likely precursor to $\mathbf{C_I}$ perhaps via dimerization or reaction with **I** to form dinuclear complexes.[11,26]

Flash photolysis (355 nm) of a *trans*-$RhCl(CO)(PPh_3)_2$ solution (0.2 mM in benzene) containing both PPh_3 (23 mM) and CO (0.72 mM) leads to formation of a transient absorbance at 410 nm largely due to $\mathbf{A_I}$. The decay of this transient was modeled with a single exponential to give $k_{obs} = (1.3 \pm 0.2) \times 10^6\ s^{-1}$. If second-order PPh_3 trapping of $\mathbf{A_I}$ to give $RhCl(PPh_3)_3$ is competitive with CO trapping to give **I**, then $k_{obs} = k_{PPh3}[PPh_3] + k_{CO}[CO]$, from which can be calculated the value $k_{PPh3} = 5.6 \pm 0.6 \times 10^7\ M^{-1}\ s^{-1}$ as an upper limit.[27] This ignores contributions of dimerization and oxidative addition pathways to the decay of transient $\mathbf{A_I}$, a valid approximation since these pathways appear to be but a minor part of the total decay (<10%) under these conditions (Scheme 2).

To evaluate whether $\mathbf{C_I}$ is a dinuclear complex, flash studies were carried out at constant laser power ($\lambda_{irr} = 355$ nm) and under low [CO] (0.13 mM) while [**I**] was systematically varied. Under these conditions the rate of the decay of $\mathbf{A_I}$ (λ_{mon} 450 nm) decreased as [**I**] decreased, e.g., at 0.3 mM $k_{obs} = (4.8 \pm 0.4) \times 10^5\ s^{-1}$, while at 0.15 mM $k_{obs} = (3.2 \pm 0.3) \times 10^5\ s^{-1}$. This behavior can be rationalized either by the reaction of $\mathbf{A_I}$ with **I**, which would be favored by higher [**I**], or by dimerization of $\mathbf{A_I}$ since higher local concentrations of $\mathbf{A_I}$ are generated because of the higher solution absorbances (Scheme 3). The latter possibility was tested by varying laser flash intensity while holding [**I**] constant (0.36 mM) in benzene at low [CO] (0.13 mM). High pump powers gave greater rates of $\mathbf{A_I}$ decay, consistent with dimerization as a major contributor to the

Scheme 3

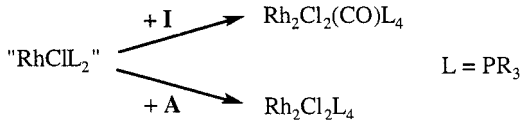

transient decay under these conditions. Thus, $\mathbf{C_I}$ is likely to be the dinuclear species $[RhCl(PPh_3)_2]_2$. If this were the only pathway, the decay curves would be expected to follow second-order kinetics behavior. However, there is a partitioning of $\mathbf{A_I}$ between dimerization, oxidative addition, and back reaction with photolabilized CO. Decays representing multiple competing processes often appear nearly exponential in character.

Despite the appearance of at least three transients in the nanosecond flash photolysis studies of **I**, long-term photolysis of **I** in deaerated solutions leads to little net reaction. Thus, all three transients must eventually follow pathways that re-form **I**. For $\mathbf{A_I}$ this would be bimolecular trapping with CO, while for $\mathbf{B_I}$ this is unimolecular, possibly reductive elimination of benzene. With regard to $\mathbf{C_I}$, previous work[11] has shown that the dimer $[RhCl(PPh_3)_2]_2$ reacts readily with CO to regenerate **I** but at rates too slow to monitor with the TRO instrumentation.

TRO Studies of I in Other Solvents. Solvent effects were probed on the UCSB instrumentation by extending the above experiments to dichloromethane, THF, and cyclohexane solutions. In CH_2Cl_2 under argon, the transient behavior was analogous to that seen in benzene, i.e., formation of a transient ($\mathbf{A_I}$) with a strong absorbance at 450 nm. This decayed exponentially under excess CO to reveal a second more weakly absorbing species ($\mathbf{B_I}$), which decayed slowly ($\sim 3 \times 10^3\ s^{-1}$) to reveal a weakly absorbing, longer lived transient ($\mathbf{C_I}$). The rate constant for the first process gave a linear k_{obs} vs [CO] (1.8−7 mM) plot analogous to Figure 4, with a slope $k_{CO} = (1.4 \pm 0.2) \times 10^8\ M^{-1}\ s^{-1}$ and an intercept of $(2.0 \pm 0.4) \times 10^5\ s^{-1}$.

If one assumes that extinction coefficients for the transients $\mathbf{A_I}$ and $\mathbf{B_I}$ are the same in dichloromethane and benzene, the flash photolysis generates higher relative concentrations of $\mathbf{B_I}$ in CH_2Cl_2. This reinforces the view that solvent oxidative addition is principally responsible for $\mathbf{B_I}$, since PPh_3 ortho-metalation rates should show minimal solvent effects. The competition between oxidative addition to give $\mathbf{B_I}$ and CO trapping of $\mathbf{A_I}$ to give **I** is again apparent from nearly 4-fold decreases in the relative yield of long-lived transients in going from argon-equilibrated solution to one that is 3.5 mM in CO.

Similar transient behavior was observed in THF (supplemental Figure S-3). Again, the initial transient absorbance did not decay completely to the baseline, and there was a modest CO-dependent residual. The k_{obs} for the initial decay was again first order with respect to [CO] (2−8 mM) with $k_{co} = (7.1 \pm 0.8) \times 10^6\ M^{-1}\ s^{-1}$ and an intercept $k_i = (2.8 \pm 0.5) \times 10^4\ s^{-1}$. In cyclohexane the dynamic behavior was similar to that seen above, although the S/N ratio was low owing to the poor solubility of **I** in this medium. The rate for the recombination of CO with transient $\mathbf{A_I}$ ($\lambda_{mon} = 450$ nm) was measured at only one [CO] (2.5 mM, $k_{obs} = 1 \times 10^6\ s^{-1}$) due to S/N problems, and $k_{co} \leq (4 \pm 2) \times 10^8\ M^{-1}\ s^{-1}$ was estimated.

The k_{CO}'s determined for the various solvents are summarized in Table 1.

TRO Studies of *trans*-$RhCl(CO)(PPh_3)_2$ (I) Using Picosecond Excitation. Argon-deaerated THF was the medium used owing to the poor solubility of **I** in cyclohexane and problems arising from multiple photon excitation of the solvent benzene. The TRO spectrum recorded 30 ps after the flash shows a broad,

(25) Oishi, S.; Kawashima, T. *Chem Lett.* **1992**, 747−750.
(26) Geoffroy, G. L.; Denton, D. A.; Keeney, M. E.; Bucks, R. R. *Inorg. Chem.* **1976**, *15*, 2382−2385.
(27) The rate constant k_{PPh3} was previously determined by competition with CO.[12] Recalculation using that data plus the k_{CO} determined here gives $k_{PPh3} = 3 \times 10^7\ M^{-1}\ s^{-1}$, nearly identical to that measured directly in the present study.

Table 1. Summary of Second-Order Rate Constants k_{CO} for the [CO]-Dependent Decay of the Principal Initial Intermediate $\mathbf{A_i}$ Generated upon 355 nm Flash Photolysis of *trans*-RhCl(CO)L_2 in Various Solvents at 23 ± 1 °C

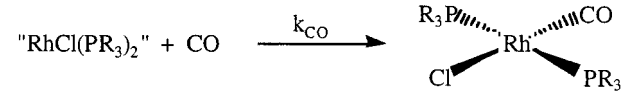

solvent	L = PPh_3, k_{CO} in 10^8 M^{-1} s^{-1}	L = P(*p*-tolyl)$_3$, k_{CO} in 10^8 M^{-1} s^{-1}	L = PMe_3, k_{CO} in 10^8 M^{-1} s^{-1}
benzene	7.8 ± 0.7	7.1 ± 0.7	12 ± 1
cyclohexane	≤ 4 ± 2[a]	6.2 ± 0.5	6.5 ± 0.8
dichloromethane	1.4 ± 0.2 (2.0 ± 0.8)[b]	4.6 ± 0.2 (3.9 ± 0.6)[b]	13 ± 2 (10 ± 5)[b]
tetrahydrofuran	0.071 ± 0.008	0.13 ± 0.4	3.7 ± 0.2

[a] Estimate based on a single concentration of CO. [b] From TRIR experiment.

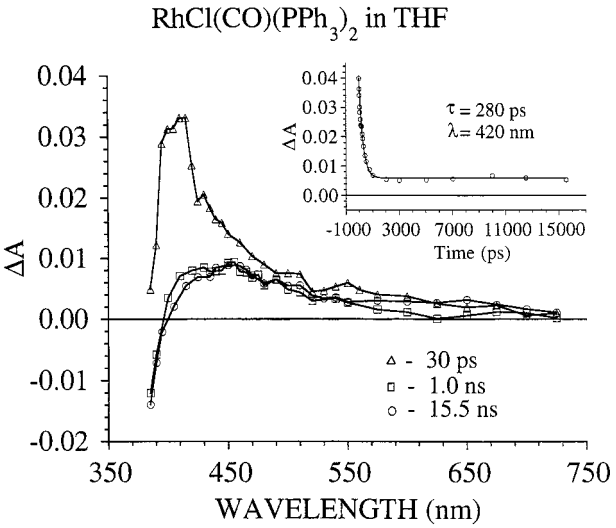

Figure 6. Transient absorbance spectra and kinetics at 420 nm recorded on the picosecond time scale for flash photolysis of a continuously flowing solution of *trans*-RhCl(CO)$(PPh_3)_3$ (**I**, 5.8 × 10^{-4} M**)** in deaerated THF solution (see Experimental Section). The transient absorbance kinetics data at 420 nm were fit to a single-exponential equation $\Delta A(t) = Ae^{-t/\tau_1} + B$, where τ_1 is a relaxation lifetime. The solid curve in the inset is a fit of the data to this equation with a lifetime of 280 ± 60 ps.

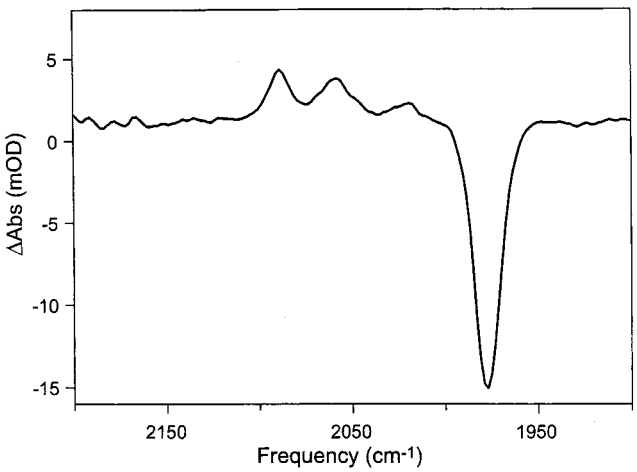

Figure 7. TRIR difference spectrum generated from the 355 nm flash photolysis of a 2 mM benzene-d_6 solution of **I**.

strong transient absorption with a maximum ΔAbs at ~420 nm (Figure 6). This decays exponentially (τ = 280 ± 60 ps) to a much longer lived species with a maximum ΔAbs at ~450 nm, the same as recorded for $\mathbf{A_I}$ above. There was no difference between spectra recorded 1 and 15 ns after the excitation pulse. In the absence of CO, these transient absorbances were very long-lived. There is evidence for an additional process after the formation of $\mathbf{A_I}$ with a lifetime of ~740 μs, leading to a long-lived residual spectrum consistent with formation of the dimer as seen above.

TRIR Studies of I. Flash photolysis (355 nm, 10 ns) in toluene led to a prompt bleaching of the ν_{CO} band of **I** at 1980 cm^{-1} and a weak transient absorption at 2023 cm^{-1}. Under CO the transient bleach decayed, but there was partial bleaching that did not undergo complete recovery on the experiment time scale, ~150 μs. The properties in CH_2Cl_2 were similar; there was an immediate bleach of the 1980 cm^{-1} band followed by a three-component decay (supplemental Figure S-4). The rate of the first component varied with [CO], whereas the second component did not, and the much slower third component could not be measured due to diffusion out of the photolysis volume. A linear k_{obs} vs [CO] (0.5−7 mM) plot for the first stage gave $k_{CO} = (2.0 \pm 0.8) \times 10^8$ M^{-1} s^{-1}, consistent with that observed in the TRO experiment in benzene. The intercept was (0.9 ± 0.1) × 10^5 s^{-1}. A transient absorption at 2020 cm^{-1} was also observed.

Similar flash photolysis experiments were carried out using the LANL step-scan FTIR instrumentation (4 cm^{-1} resolution). A transient difference spectrum was generated using a 0−100 μs window after 355 nm flash photolysis of **I** (2 mM) in deaerated benzene-d_6. This displayed a bleach of the parent ν_{CO} band at 1980 cm^{-1} and distinct transient absorbances at 2060 and 2085 cm^{-1} and a weaker absorbance at 2020 cm^{-1} (Figure 7). The two stronger absorption bands occur at frequencies consistent with those expected for a Rh(III) carbonyl complex, i.e., the product of oxidative addition.

TRO Studies of *trans*-RhCl(CO)(P(*p*-tolyl)$_3$)$_2$ (II). The TRO behavior of **II** in benzene solution after 355 nm pulsed (10 ns) excitation is closely analogous to that of **I**, exhibiting multi-component decay of species $\mathbf{A_{II}}$, $\mathbf{B_{II}}$, and $\mathbf{C_{II}}$ when monitored at 450 nm. Under argon, $\mathbf{A_{II}}$ appeared to decay via mixed order kinetics to a residual ΔAbs ($\mathbf{B_{II}}$) that decayed much more slowly, leaving a residual absorbance ($\mathbf{C_{II}}$) that was longer lived than the TRO detection limits (~50 ms). Under excess CO, decay of $\mathbf{A_{II}}$ followed first-order kinetics independent of λ_{mon} (410−550 nm). A plot of k_{obs} vs [CO] (0.5−6 mM) proved linear, with $k_{co} = (7.1 \pm 0.7) \times 10^8$ M^{-1} s^{-1} and an intercept of $(1.0 \pm 0.3) \times 10^5$ s^{-1}. Furthermore, the relative yield of the longer lived transients $\mathbf{B_{II}}$ and $\mathbf{C_{II}}$ (defined in Figure 5) decreased from ~28% with no added CO to ~2.5% at [CO] > 4 mM. Thus, $\mathbf{A_{II}}$ has the behavior expected for the tricoordinate species "$RhClL_2$" and $\mathbf{B_{II}}$ appears to be largely formed from $\mathbf{A_{II}}$ in competition with CO trapping. The disappearance of $\mathbf{B_{II}}$ could be fit to a monoexponential decay with $k_{obs} = (1.6 \pm 0.4) \times 10^3$ s^{-1}, independent of [CO]. Supplemental Figure S-5

displays the spectrum of **II** and transient spectra recorded 50 ns ($\mathbf{A_{II}}$) and 50 μs ($\mathbf{B_{II}}$ plus $\mathbf{C_{II}}$) following flash photolysis of *trans*-RhCl(CO)(P(*p*-tolyl)$_3$)$_2$ in benzene under CO (6.7 mM).

Solvent effects were qualitatively the same as seen above for **I**. The k_{CO} values obtained from linear plots of k_{obs} vs [CO] were $(4.6 \pm 0.4) \times 10^8$ M^{-1} s^{-1} in CH_2Cl_2 and $(6.2 \pm 0.5) \times 10^8$ M^{-1} s^{-1} in cyclohexane but much smaller, $1.3 \pm 0.4 \times 10^7$ M^{-1} s^{-1}, in THF (Table 1). The CO-independent terms (the intercepts) were $(1.0 \pm 0.5) \times 10^5$ s^{-1} and $(2.0 \pm 0.4) \times 10^4$ s^{-1} in dichloromethane and THF. The decay of $\mathbf{B_{II}}$ displayed a rate constant of 3×10^3 s^{-1} in CH_2Cl_2, but the low signal/noise ratio prevented following this in cyclohexane.

TRO Studies of II Using Picosecond Excitation. The picosecond studies in deaerated THF also gave results closely analogous to those for **I**. Flash photolysis led to prompt (<30 ps) formation of a strong transient absorption with a ΔAbs maximum at ~420 nm. This was followed by rapid exponential decay (τ ~560 $\pm$ 60 ps) to a transient difference spectrum (a broad ΔAbs maximum at ~460 nm) consistent with that of $\mathbf{A_{II}}$ and having a lifetime $\gg$15 ns.

TRIR Studies of *trans*-RhCl(CO)(P(*p*-tolyl)$_3$)$_2$ (II). Flash photolysis (355 nm) of **II** (1 mM) in dichloromethane led to temporal bleaching of the parent ν_{CO} band at 1974 cm^{-1} followed by a three-component decay similar to that seen for **I**. The rate for the first component was [CO] dependent, with a k_{CO} value ($(3.9 \pm 0.6) \times 10^8$ M^{-1} s^{-1}) nearly identical to that determined in the TRO experiment. The decay of $\mathbf{B_{II}}$ was CO independent ($(1.5 \pm 0.5) \times 10^3$ s^{-1}), and the third component could not be measured due to diffusion/flow out of the probe volume. There was little net photoreaction, as evidenced by the unchanged solution spectrum after repetitive flashes (1000 shots at 2 Hz).

Flash photolysis of **II** (~1 mM) in benzene-d_6 gave step-scan FTIR results similar to those observed for **I**. A strong bleach of the parent ν_{CO} at 1975 cm^{-1} and weaker transient absorption bands at 2085, 2060, and 2020 cm^{-1} were observed in the 0−100 μs window after the flash.

TRO Studies of *trans*-RhCl(CO)(PMe$_3$)$_2$ (III). When a benzene solution of **III** (0.25 mM) was subjected to 355 nm flash photolysis (10 ns), the difference spectrum displayed prompt formation of $\mathbf{A_{III}}$ with a broad absorption from 390 nm to ~650 nm (ΔAbs maximum at 410 nm). This decayed to another, much longer lived (>50 ms) transient $\mathbf{B_{III}}$, which was too long-lived to follow its decay. Analogous behavior was seen when the transient bleach was monitored at 380 nm. Under argon, the decay of $\mathbf{A_{III}}$ was of mixed order, but under added CO this was pseudo-first-order. A plot of k_{obs} vs [CO] (0.05−0.7 mM) was linear, giving $k_{CO} = (1.2 \pm 0.2) \times 10^9$ M^{-1} s^{-1} with an intercept of $(1.5 \pm 0.8) \times 10^5$ s^{-1}. Similar transient kinetics were observed in cyclohexane, CH_2Cl_2, and THF, and the respective k_{CO} values were $(6.5 \pm 0.8) \times 10^8$, $(1.3 \pm 0.2) \times 10^9$, and $(3.7 \pm 0.2) \times 10^8$ M^{-1} s^{-1} (Table 1). (The respective intercepts were $(5.1 \pm 1.0) \times 10^5$, $(3.5 \pm 2.0) \times 10^5$, $(1.7 \pm 0.4) \times 10^4$ s^{-1}.) Notably, k_{CO} in THF is only a factor of 3 smaller than in benzene, in contrast to the observations with $\mathbf{A_I}$ and $\mathbf{A_{II}}$, where solvent effects are much larger.

Figure 8 illustrates the TRO spectra immediately (0−400 ns) after and 18−20 μs after 355 nm flash photolysis of **III** in argon-deaerated benzene containing 0.42 mM PMe$_3$. The initial spectrum is that of $\mathbf{A_{III}}$. This undergoes exponential decay to reveal a new long-lived transient with spectral properties consistent with formation of RhCl(PMe$_3$)$_3$ (eq 3). A plot of k_{obs} vs [PMe$_3$] (0.2 to 1.0 mM) is linear with a slope (k_{PMe3}) of $(1.1 \pm 0.2) \times 10^9$ M^{-1} s^{-1} and an intercept of $(1.5 \pm 0.5) \times 10^4$ s^{-1}.

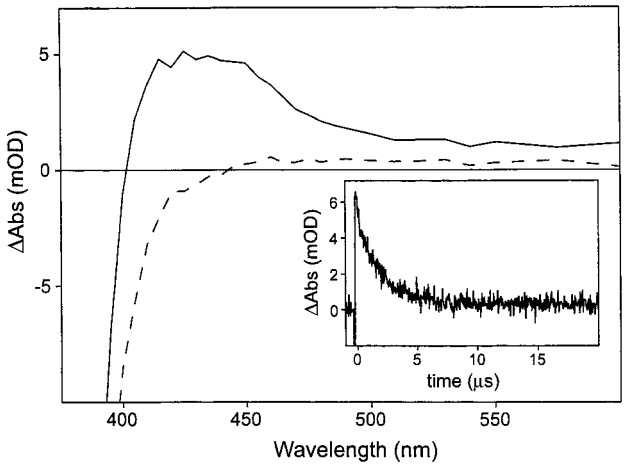

Figure 8. Transient spectra from the flash photolysis of *trans*-RhCl(CO)(PMe$_3$)$_2$ in the presence of added PMe$_3$.

$$\mathbf{A_{III}} + \mathrm{PMe_3} \xrightarrow{k_{PMe3}} \mathrm{RhCl(PMe_3)_3} \qquad (3)$$

TRO Studies of III Using Picosecond Excitation. The picosecond flash studies of **III** in deaerated THF revealed a more complicated scenario than seen for **I** and **II**. Again, a transient is formed promptly (<30 ps) with a maximum ΔAbs at ~390 nm. This relaxed over ~15 ns to the transient difference spectrum (maximum ΔAbs ~410 nm) for $\mathbf{A_{III}}$ described above in the nanosecond flash photolysis studies. However, the course of this decay reveals at least two components (supplemental Figure S-6), one very short (~70 ps) and the second a factor of 40 longer (~2.5 ns). Analogous studies in cyclohexane gave similar behavior but with somewhat different relaxation times (~40 ps and ~5.5 ns, respectively). Longer time frame observation in THF showed at least two more decay processes, one occurring on the 10−100 ns time scale, the other on a 180 μs time scale leading to a residual difference spectrum. The species giving the residual spectrum are not known, although the dimer [RhCl(PMe$_3$)$_2$]$_2$ and oxidative addition products are likely candidates (see below).

Low-Temperature FTIR Studies of *trans*-RhCl(CO)(PMe$_3$)$_2$ (III). When 213 K THF/benzene (5:1 v/v) solutions of **III** were subjected to continuous photolysis at $\lambda_{irr} > 300$ nm, the resulting FTIR spectrum showed bleaching of the1962 cm^{-1} ν_{CO} band for the parent and the appearance of a broad band at 2070 cm^{-1} with a shoulder about half as intense at 2050 cm^{-1} (supplemental Figure S-7). Other bands, less than one-fourth the intensity of the 2070 cm^{-1} band, were visible at 2130 and 2018 cm^{-1}. These spectral changes displayed an indefinitely long lifetime at 213 K. The new bands are consistent with the ν_{CO} values expected for Rh(III)-coordinated CO. Rhodium−hydride stretches ν_{RhH} of related compounds fall in the same frequency range.[28] The band at 2130 cm^{-1} is coincident with that expected for free CO, but the relative intensity appears too large for that species alone.[29] When the photolysis was carried out in perdeuterio solvent, the bleach at 1962 cm^{-1} was accompanied by appearance of only one new absorption, a strong ν_{CO} band at 2050 cm^{-1}, broad in a manner suggesting two overlapping bands. This suggests that the absorbances appearing for the photoproduct in perprotio benzene at 2130

(28) (a) Kaesz, H. D.; Saillant, R. B. *Chem. Rev.* **1972**, *72*, 231−281. (b) Intille, G. M. *Inorg. Chem.* **1972**, *11*, 695−702.

and 2018 cm^{-1} are ν_{RhH} bands, while the two seen at 2070 and 2050 cm^{-1} represent ν_{CO} bands for a pair of monocarbonyl products. This is in agreement with the earlier NMR studies which concluded that two Rh(III) isomers (**X** and **Y**) were formed in comparable concentrations upon photolysis of **III** under analogous low-temperature conditions.[7d,9a,30] The modest frequency shift(s) for the ν_{CO} bands in C_6D_6 relative to the perprotio medium may reflect coupling to a Rh−H of comparable frequency in the latter system.[31]

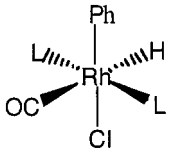

X

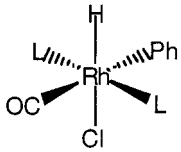

Y

TRIR Studies of III. Temporal IR absorbance changes following 355 nm excitation of **III** in benzene were monitored using a tunable single-frequency probe source set at 2070 cm^{-1}. Two processes were evident, prompt rise within the time constant of the instrument (<100 ns) and a "delayed" rise of comparable intensity which could be fit to a first-order rate law with a $k_{obs} = (1.0 \pm 0.1) \times 10^5\ s^{-1}$. The first-order nature of the slow rise suggests that oxidative addition is the rate-limiting step for the formation of $RhCl(CO)(PMe_3)_2(Ph)(H)$, not the second-order reaction of $RhCl(PMe_3)_2(Ph)(H)$ with CO (see below). When the analogous experiment was carried out under 0.7 mM CO, the prompt rise at 2070 cm^{-1} remained, but the slower first-order rise was quenched, indicating that the species responsible for the delayed process was trapped by CO. However, there were some ambiguities in the quantitative observation of prompt formation of the 2070 cm^{-1} peak depending on the photochemical history of the solutions which frustrated attempts to quantify this signal.[32]

TRIR experiments using the step-scan technique demonstrated that 355 nm flash photolysis of **III** in benzene-d_6 solution under argon leads to a transient difference spectrum fully consistent with that seen for low-temperature FTIR experiments in this medium. A strong transient bleach at 1962 cm^{-1} and a new, broad absorbance at 2050 cm^{-1} corresponding to the formation of an intermediate were observed (supplemental Figure S-8).[1c] The "delayed" rise of the absorbance at 2050 cm^{-1} could be fit to a first-order rate law with a $k_{obs} = (8 \pm 1) \times 10^4\ s^{-1}$ at 23 °C. The analogous pathway in benzene gave $k_{obs} = (1.0 \pm 0.1) \times 10^5\ s^{-1}$, indicating a modest normal kinetic isotope effect ($k_h/k_d \sim 1.3 \pm 0.3$) as is often found with oxidative additions.[33]

Calculations on the Model Compound *trans*-RhCl(CO)-$(PH_3)_2$. Ab initio calculations with the COLUMBUS programs,[23] using the relativistic effective core potentials and spin−orbit operators of Christiansen et al.,[34] were performed on the model complex *trans*-$RhCl(CO)(PH_3)_2$ in C_{2v} symmetry. A ground state electronic configuration was computed using bond lengths reported for the structure[35] of **I** but with P−Rh−P and Cl−Rh−C bond angles set at 180°. The calculated highest occupied molecular orbital has a_1 symmetry and is 88% rhodium in character, largely a linear combination of $d_{x^2-y^2}$ and d_{z^2} orbitals. Other proximal occupied MO's are largely Rh-d in character. The two lowest unoccupied MO's have b_1 and b_2 symmetry and are principally C-p and O-p orbitals of the carbonyl group with some admixture of Rh-p orbitals. Also grouped among the lowest energy unoccupied MO's is an a_1 orbital largely Rh-$d_{x^2-y^2}$ in character. Thus, the HOMO-to-LUMO transition is indicated to be metal-to-ligand (CO) charge transfer (MLCT) in character, consistent with previous assignments for lower energy bands of *trans*-$RhCl(CO)L_2$ complexes.[36]

Franck−Condon (vertical) excited state (ES) energies were calculated as open shell states without nuclear relaxation by moving an electron from an occupied orbital to an unoccupied orbital without optimizing the excited state geometry. Limitations of these calculations were that for a given occupied-to-unoccupied MO excitation, and symmetry for only the lowest energy singlet and triplet states could be calculated. Since the ground state had $^1A_1$ symmetry, no $^1A_1$ ES could be calculated, although the lowest energy $^3A_1$ state (a ligand field state) could be. The lowest energy singlet and triplet MLCT ES could be computed, as they have B_1 symmetry. Excited state energies were computed at fixed Rh−CO bond distances, and potential surface diagrams were generated by systematically varying only this parameter and fitting the results to a Morse potential (Figure 9). The $^1A_1$ ground state has a calculated bond dissociation energy of 45 kcal mol^{-1}, surprisingly close to the Rh−CO bond dissociation energy of 48.2 kcal/mol reported for *trans*-$RhCl(CO)(P^iPr_3)_2$ (P^iPr_3 is tris(2-propyl)phosphine).[37] The ^{3}MLCT states are bound states with large Rh−CO bond dissociation energies; however, a triplet ligand field state ($^3A_1$) of comparable energy is dissociative with respect to the Rh−CO bond. The latter is computed to correlate with the ground electronic state for a T-shaped tricoordinate intermediate once CO is fully

(29) (a) Free CO has a reported extinction coefficient of ~400 $M^{-1}cm^{-1}$ at 2132 cm^{-1} in a 77 K 3-methylpentane matrix,[29a] although the value in room-temperature benzene is very small (17 $M^{-1}\ cm^{-1}$).[29b] With this in mind, the band observed at 2130 cm^{-1} might be due to the free CO instead of a Rh−H stretch. To address this possibility, an estimate of the ΔAbs expected at 2130 cm^{-1} based upon the transient bleaching of the ν_{CO} of **III** gives a significantly smaller value for the expected absorption at that frequency even if CO were the only CO-containing photoproduct generated under the conditions. (b) Bentsen, J. G.; Wrighton, M. S. *J. Am. Chem. Soc.* **1984**, *106*, 4041−4043. (c) This work.

(30) (a) Bitterwolf and co-workers[30b] observed a band of several different transient FTIR absorptions in the ν_{CO} region following CW photolysis of solid **III** in Nujol mulls at low temperature and have assigned bands at 1938 cm^{-1} to $RhCl(CO)(PMe_3)_3$, at 1955 cm^{-1} (weak) to $RhCl(CO)PMe_3$, and at 2012 cm^{-1} to *cis*-$RhCl(CO)(PMe_3)_2$. We have no ready explanation of these differences except to comment that we are confident of the validity of the results reported here for the low-*T* glassy solutions which agree qualitatively with the ambient-temperature TRIR and step-scan FTIR results also described. (b) Bitterwolf, T. E. Private communication, reported at several National ACS meetings.

(31) (a) An earlier study[31b] of isotope effects on the infrared spectra of the metal carbonyl hydride/deuteride anions $(H/D)M(CO)_4^-$ (M = Fe, Ru, or Os) demonstrated shifts up to 41 cm^{-1} of certain ν_{CO} frequencies upon replacing H with D. (b) Walker, H. W.; Ford, P. C. *Inorg. Chem.* **1982**, *21*, 2509−2510.

(32) Studies were undertaken to ascertain the effect of varying the intensity of the excitation pulse on the prompt formation of the 2070 cm^{-1} transient. The prompt signal was seen in every case, and that signal increased in a roughly linear correspondence with pump power. However, solutions that had been recently subjected to flash photolysis displayed a larger prompt signal even though the TRIR spectra showed no new bands in the carbonyl region, indicative of other photoactive species being formed in the initial excitation. The same solutions allowed to age for a few hours behaved in the same manner as freshly prepared solutions.

(33) Zhou, P.; Vitale, A. A.; Filippo, J. S., Jr.; Saunders, W. H., Jr. *J. Am. Chem. Soc.* **1985**, *107*, 8049−8054.

(34) (a) Christiansen, P. A.; Ermler, W.; Pitzer, K. S. *Annu. Rev. Phys. Chem.* **1985**, *36*, 407−32. (b) Ermler, W. C.; Ross, R. B.; Christiansen, P. A. *Adv. Quantum Chem.* **1988**, *19*, 139−82.

(35) Ceriotti, A.; Ciani, G.; Sironi. *J. Organomet. Chem.* **1983**, *247*, 345−350.

(36) Geoffroy, G. L.; Wrighton, M. S.; Hammond, G. S.; Gray, H. B. *J. Am. Chem. Soc.* **1974**, *96*, 3105−3106. Geoffroy, G. L.; Isci, H.; Litrenti, J.; Mason, W. R. *Inorg. Chem.* **1977**, *16*, 1950−1955.

(37) Wang, K.; Rosini, G. P.; Nolan, S. P.; Goldman, A. S. *J. Am. Chem. Soc.* **1995**, *117*, 5082−5088.

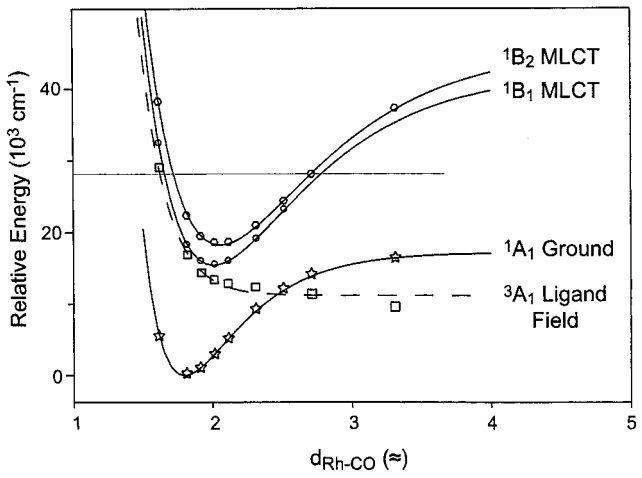

Figure 9. Potential curves derived from ab initio calculations of ground and one-electron excited states of *trans*-RhCl(CO)$(PH_3)_2$.

dissociated (with other bond lengths and angles held at those of the model starting complex).

Discussion

Nature of A_i (i = I, II, or III). Several results described above identify $\mathbf{A_i}$ as the "$RhClL_2$" product of CO photolabilization from *trans*-RhCl(CO)L_2 (eq 2). First, in each solvent system probed by TRO experiments, the lifetime of $\mathbf{A_i}$ is markedly attenuated by added CO, and the resulting spectral changes were consistent with the regeneration of **I**, **II**, or **III**, respectively. The lifetime of $\mathbf{A_i}$ was also attenuated by added L, but product spectra were those of the tris(phosphine) species $RhClL_3$, clearly different from the starting complexes. Thus, CO labilization (eq 2), not PR_3 labilization, is the principal photoreaction pathway.

The TRIR data are in accord with this conclusion. For example, photoexcitation of *trans*-RhCl(CO)$(PPh_3)_2$ led to bleaching of the ν_{CO} band at 1980 cm^{-1} in the TRIR spectra, and the [CO]-dependent kinetics of that band's regeneration gave the same k_{CO} as determined in the TRO experiments. While such observations do not exclude low quantum yield Cl^- or L dissociation, these are at most minor pathways.[38]

Is A_i Solvated, or Is It Tricoordinate? Comparisons of the transient difference spectra representing the various $\mathbf{A_i}$ in different media (e.g., Figure 1) show modest solvent shifts. However, this can hardly be considered diagnostic, since such shifts can result from bulk solvent effects on the charge transfer bands from which the difference spectra are constructed. Nonetheless, we propose that these species are four-coordinate with the solvent occupying the position vacated by the labilized CO, the intermediate being lightly stabilized by poorer donor solvents such as benzene, dichloromethane, and cyclohexane and more strongly coordinated by the donor THF. Square planar d^8 complexes generally undergo substitution reactions by associative pathways, and the small $\Delta H^{\ddagger}$ and negative $\Delta S^{\ddagger}$ for the reaction of CO with $\mathbf{A_I}$ in benzene are in accord with such a mechanism. Leaving group effects are likely to be minor if the ligand is but weakly coordinated, so the significantly decreased reactivity toward CO in THF points convincingly to a solvento complex, RhCl(Sol)L_2, in that medium.

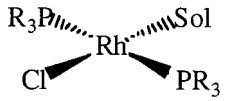

Sol = Solvent

The "tricoordinate" species $RhCl(P^iPr_3)_2$ has been used as a starting material in synthesis schemes.[39] In the solid state this was characterized as a dimer, but in hydrocarbon solution it is monomeric, very likely stabilized as the solvento species. An alternative to solvento stabilization might be agostic interaction with a C−H bond of L, especially if L is a triaryl phosphine. In this context, Reed et al.[40] have reported preparation of the solvento complexes $[Rh(PPh_3)_3(Sol)](ClO_4)$, where Sol is an oxygen donor such as an alcohol, ether, or acetone. Recrystallization from CH_2Cl_2 gave the salt of the tricoordinate cation $[Rh(PPh_3)_3^+]$, which was characterized structurally. The phosphines have a planar, nearly T-shaped, coordination about the Rh(I). The fourth coordination site appears to be involved in an interaction with one of the ligand phenyl groups, as evidenced by an acute Rh−P−Ph angle which brings the phenyl C-1, C-2, and ortho-H within attractive distances to the metal (2.48, 2.62, and ~2.56 Å, respectively).

Solvento intermediates are also concluded to form following CO photodissociation from $CpRh(CO)_2$ ($Cp = \eta^5$-C_5H_5)[41] and Tp*Rh$(CO)_2$ (Tp* = HB(3,5-dimethylpyrazolyl),[42] both systems known to activate hydrocarbon C−H bonds. For example, ultrafast flash photolysis (100 fs time resolution) of $CpRh(CO)_2$ in cyclohexane gave a monocarbonyl complex with spectral properties attributed to the solvated intermediate CpRh(CO)-(cyclohexane). Even on this time scale, the naked CpRh(CO) precursor to the solvento species was not seen.[41] The monocarbonyl solvento complex was identified as the precursor to C−H activation in both pulsed and continuous photolysis studies of Tp*Rh$(CO)_2$.[42,43]

Other considerations with regard to the structure of $\mathbf{A_i}$ arise from density functional calculations by Ziegler et al. on the tricoordinate model $RhCl(PH_3)_2$ in the absence of solvent interactions.[10b] These concluded that the cis and trans T-shaped isomers should be in labile equilibrium (eq 4), the cis being the more stable. This conclusion parallels our earlier suggestion[1d] that cis intermediates might be playing a role in the photochemistry of **III** (see below). (Given the steric bulk of the triarylphosphines, cis T-shaped isomers are less likely in reactions of **I** or **II**.) However, the reaction of $\mathbf{A_{III}}$ with CO regenerates a product with the same ν_{CO} as the starting complex, so if $\mathbf{A_{III}}$ includes a significant fraction of the cis isomer, the ambient temperature reaction with CO would require concerted cis-to-trans rearrangement. This seems unlikely, since substitution reactions of d^8 square planar complexes are generally stereoretentive. Furthermore, the isomeric oxidative addition products **X** and **Y** each have trans phosphines.[9a] Thus we conclude, that if the cis, T-shaped isomer is formed upon CO photolabilization from **III**, it is short-lived and isomerizes to the trans analogue prior to trapping with CO or oxidative addition of solvent (see below).

(38) (a) The demonstration that the $CF_3SO_3^-$ anion resists labilization in a dichloromethane solution of *trans*-Rh(CF_3SO_3)(CO)$(PPh_3)_2$ even when a donor ligand such as H_2O is present argues against the photolabilization of Cl^- in the present systems. (b) Svetlanova-Larson, A.; Hubbard, J. L. *Inorg. Chem.* **1996**, *35*, 3073−3076.

(39) Rappert, R.; Nürnberg, O.; Werner, H. *Organometallics* **1993**, *12*, 1359−64.
(40) Yared, Y. W.; Miles, S. L.; Bau, R.; Reed, C. A. *J. Am. Chem. Soc.* **1977**, *99*, 7076−7078.
(41) Asbury, J. B.; Ghosh, H. N.; Yeston, J. S.; Bergman, R. G.; Lian, T. *Organometallics* **1998**, *17*, 3417−3419.
(42) Bromberg, S. E.; Yang, H.; Asplund, M. C.; Lian, T.; McNamera, B. K.; Kotz, K. T.; Yeston, J. S.; Wilkens, M.; Bergman, R. G.; Harris, C. B. *Science* **1997**, *278*, 260−263
(43) Purwoko, A. A.; Lees, A. J. *Inorg. Chem.* **1996**, *35*, 675−682.

(4)

Nature of B_i (I = I, II, or III). Several observations identify B_i being the product of oxidative addition to an activated Rh(I) complex. The most convincing are NMR studies[9] that demonstrated the photolysis products of *trans*-RhCl(CO)$(PMe_3)_2$ in 230 K benzene/THF (1:3, v/v) to be the hexacoordinate RhCl(CO)$(PMe_3)_2$(H)(Ph) isomers **X** and **Y** plus *trans*-RhCl(Ph)$(PMe_3)_2$, products of benzene oxidative addition. Complementary experiments described here are the TRIR, step-scan FTIR, and low-temperature FTIR studies. Photolysis of **III** in low-temperature benzene/THF leads to the appearance of two higher frequency ν_{CO} bands which can be attributed to the carbonyls of **X** and **Y** as well as several additional (weaker) bands consistent with Rh−H stretches. The latter assignment is especially attractive given that these bands were not observed when the photolysis was carried out in benzene-d_6. The step-scan FTIR experiments confirmed that analogous spectral change results in ambient-temperature benzene-d_6 solutions of **III** when subjected to flash photolysis.

Step-scan FTIR spectra also demonstrated that photolysis of the Ph_3P complex **I** in benzene-d_6 leads to bleaching of the parent ν_{CO} band accompanied by transient absorptions at higher frequencies consistent with oxidative addition products. The apparent yield (gauged by relative band intensities) is much smaller than for **III** under comparable conditions.

How Does B_I Form, and What Happens Next? Scheme 4 portrays possible scenarios for B_i formation and decay. The substantial CO quenching of B_i formation seen in the TRO experiments indicates that A_i is the origin of much of the oxidative addition chemistry observed in the absence of added CO. This is confirmed by the time-dependent increase of the 2070 cm^{-1} absorption in the TRIR experiments with *trans*-RhCl(CO)$(PMe_3)_2$ in benzene under argon, which we attribute to rate-limiting C_6H_6 oxidative addition to A_{III} followed by rapid coordination of CO to give B_{III}. This behavior was repeated in all the solvents studied and is in conflict with a conclusion based on a continuous photolysis study[44] that C−H activation in cycloalkanes occurred from species such as A_i but at a rate too fast for the trapping by CO to be competitive.

Notably, the TRO experiments also demonstrated that a fraction of the formation of B_i was not quenched by added CO; thus it must be formed by a pathway independent of A_i for each of the *trans*-RhCl(CO)L_2 complexes. This is consistent with proposals[7d,9d] that the oxidative addition photoproducts **X** and **Y** result from direct reactions of the electronic excited state prepared by the initial excitation of **III**. Our earlier report[1c] that a component of the IR absorption at 2070 cm^{-1} formed promptly (<100 ns) according to the TRIR experiments also supports this proposal. However, as noted above,[32] attempts to quantify the prompt fraction of that signal were frustrated by finding that this is influenced by the solution history. Despite the ambiguity, however, both the TRIR and the nanosecond TRO experiments clearly demonstrate that the formation of B_I involves two pathways, one that proceeds by formation of A_i and is quenchable by added CO and one that is *not* so quenched.

On the picosecond time scale, TRO experiments with **I** and **II** demonstrate initial formation of short-lived species, $\tau = \sim 280$ ps and ~560 ps, which are apparently the predecessors of A_I and A_{II}, respectively. These may be electronic excited states, which decay nonradiatively to the ground states in competition with CO dissociation to give A_I and A_{II} with quantum efficiencies of about 10%.[7d] A lifetime of this magnitude is reasonable if the lowest energy ESs of these complexes are ^{3}MLCT states, as suggested by the calculations (Figure 9). Ligand field excitation of metal carbonyls often leads to CO labilization on time scales < 1 ps and with quantum yields approaching unity in fluid solutions.[45] In the present case, the quantum yields are much smaller, so the lowest energy ES must be sufficiently long-lived for nonradiative decay to become the predominant deactivation mechanism. CO labilization might then result from crossing from the ^{3}MLCT ES to the dissociative ligand field state ($^3A_1$) calculated to be energetically close. An alternative assignment of these short-lived transients could be tricoordinate species which decay by coordination and vibronic relaxation to the solvento complexes; however, such relaxation processes should be much faster than the observed processes.

Scheme 4

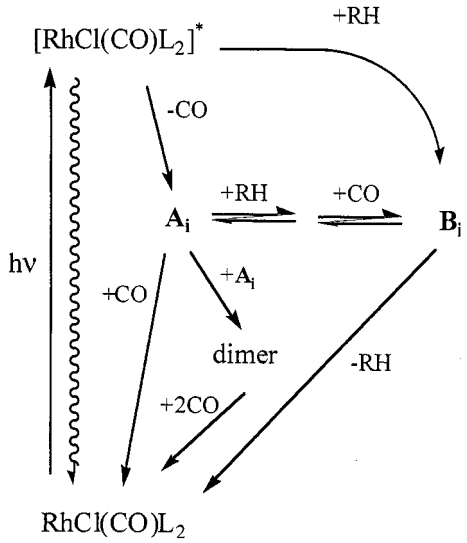

Somewhat different behavior was seen in the picosecond TRO experiments with **III**, i.e., two short lifetime processes are apparent. The shorter of these with $\tau = \sim 70$ ps in THF and ~40 ps in cyclohexane fall closer to the time frames expected for solvent coordination/vibronic relaxation of an intermediate generated by CO photodissociation. However, the spectroscopic similarity of this species to the initial transients observed in the picosecond flash photolyses of **I** and **II** argues that all three are analogous. A likely scenario is that this is also a ^{3}MLCT excited state. The more puzzling observation is the second process seen for **III**, which has lifetimes of ~2.5 ns in THF and ~5.5 ns in cyclohexane but is not seen for either **I** or **II**. The time frame is certainly too long to represent solvent capture and vibrational relaxation of an unsaturated intermediate created by CO dissociation. One possibility is the cis/trans isomerism of the tricoordinate intermediate $RhClL_2$ proposed by Ziegler, since the smaller stereochemical demands of PMe_3 ligands in **III** would favor the cis isomer more than the triaryl phosphine ligands in **I** and **II**. It was argued above that the A_{III} species involved in benzene activation and in CO trapping to give **III** was likely to have the trans geometry. If so, then the additional

(44) Rosini, G. P.; Soubra, S.; Vixamar, M.; Wang, S.; Goldman, A. S. *J. Organomet. Chem.* **1998**, *554*, 41−47.

(45) Reviewed by Ford, P. C.; Boese, W.; Lee, B.; McFarlane, K. L. In *Photosensitization and Photocatalysis by Inorganic and Organometallic Compounds*; Graetzel, M., Kalyanasundaram, K., Eds.; Kluwer Academic Publishers: The Netherlands, 1993; pp 359−390.

relaxation process seen in the picosecond experiments may represent decay of a cis-isomer also formed in the flash photolysis of **III**.

In summary, nanosecond and picosecond TRO spectroscopic studies combined with both step-scan FTIR and point-by-point TRIR spectral experiments have been described for three rhodium(I) phosphine complexes *trans*-RhCl(CO)L_2. After 355 nm excitation, all three display a short-lived transient concluded to be a MLCT excited state, which decays to a second species concluded to be the solvated product of CO labilization *trans*-RhCl(Sol)L_2 ($\mathbf{A_I}$). When L = PMe_3, there is an additional short-lived (<10 ns) species speculated to be the cis analogue. $\mathbf{A_i}$ was demonstrated to undergo trapping by CO to re-form the respective *trans*-RhCl(CO)L_2 complexes competitive with a first-order process to form $\mathbf{B_i}$ concluded to be the hexacoordinate product of solvent oxidative addition. However, there is also an unquenchable component of $\mathbf{B_i}$ formation, which led to the conclusion that oxidative addition products are also being formed promptly upon photoexcitation of the starting complex, either by direct reaction of the electronic excited state with solvent or by reaction of a vibrationally hot species (either *trans*-RhCl(CO)L_2 or $RhClL_2$) formed upon decay of the excited state. The absence of significant net reactions after repeated pulse photolysis shows that, under these conditions, there is no net photodecomposition or other pathways depleting *trans*-RhCl(CO)L_2. The TRO and TRIR techniques have also been able to determine the rates of the reactions of L and of CO with $\mathbf{A_i}$ (to form $RhClL_3$ and *trans*-RhCl(CO)L_2, respectively) and to demonstrate the effects of solvent and the identity of L upon the kinetics for these species relevant to photocatalytic C−H activation.

Acknowledgment. This research was sponsored by a grant (DE-FG-03-85ER13317) to P.C.F. from the Division of Chemical Sciences, Office of Basic Energy Sciences, U.S. Department of Energy, and by a Collaborative UC/Los Alamos Research (CULAR) Initiative grant from Los Alamos National Laboratory. We thank C. T. Spillett (UCSB), W. T. Boese (UCSB), D. B. Pourreau (Amoco), B. L. Lee (UCSB), and S. Bernhard (LANL), who each contributed to the accumulation of experimental data described here, and J. A. Simon (UCSB) for help with ab initio calculations. We thank Johnson-Matthey, Inc. for a loan of the $RhCl_3 \cdot 3H_2O$ used in syntheses.

Supporting Information Available: Eight supplemental figures. This material is available free of charge via the Internet at http://pubs.acs.org.

IC001298X